PIER M

(Received 1 December 2025, Accepted 2 February 2026, Scheduled 31 March 2026)

Adaptive Metaheuristic Optimization of New Dynamic Preisach Hysteresis Modeling

Ahmed Nait Ouslimane[1], Yasmine Gabi[2, 3, *], Kevin Jacob[2, 3], and Bernd Wolter[3]

[1] *Department of Electrotechnics, Mouloud Mammeri University Tizi-Ouzou 15000, Algeria*
[2] *Chair of Cognitive Sensor Systems, Saarland University, Campus E3 1, 66123 Saarbrücken, Germany*
[3] *Fraunhofer Institute for Nondestructive Testing IZFP, Campus E3 1, 66123 Saarbrücken, Germany*

ABSTRACT: This study presents a method which improves the accuracy of Preisach model that is able to reproduce the magnetic response of ferromagnetic material to change of magnetic fields, especially at higher frequency. The approach consists in extending an existing model and uses mathematical tools like combining a closed-form Everett function for hysteresis modeling with the Monte Carlo integration method to approximate the Preisach function, making calculations faster and more reliable. To find the best settings for the model, two optimization techniques are used: genetic algorithms (GA) and artificial bee colony (ABC). The model is tested by comparing its predictions to real-world experimental data, and it shows excellent accuracy and efficiency. Between the two techniques, GA performs better in terms of precision and reliability, making it a good choice for solving complex problems in modeling magnetic behavior.

1. INTRODUCTION

For several decades, the design of new materials and advanced machines has aimed for high technological performance, focusing on critical aspects such as energy efficiency, miniaturization, integration, and the ability to withstand diverse operating conditions, including various waveforms, frequencies, and temperatures. Electrical engines often face numerous challenges that highlight the central role of materials in the development of robust prototypes.

This investigation seeks to design and optimize resilient machines by concentrating on the initial stages of the predesign and exploration of virtual prototypes. The objective is to analyze the behavior of the material in the context of the development of large magnetic machines while considering external factors. To achieve this, it is essential to utilize reliable models for designing ferromagnetic engines that can accurately simulate realistic behavior under specific conditions, such as different operating points, amplitudes, and frequencies. Accurate modeling and parameter identification of hysteresis loops are crucial for the simulation and design of electromagnetic sensors [1, 2].

Modeling magnetic hysteresis under dynamic excitation is challenging because of the intrinsic nonlinearity, history dependence, and rate sensitivity of soft magnetic alloys. A variety of hysteresis modeling approaches have been reported in the literature. The Jiles and Atherton model is popular for its physical interpretability and computational efficiency, with recent adaptations, including frequency-dependent and physics-guided deep learning extensions, improving its dynamic accuracy [3, 4]. Zirka et al. introduced dynamic adaptations to address frequency and rate-dependent magnetization behavior [5]. Recent reviews have highlighted that only rate-aware models, which incorporate time derivatives and viscosity-like behavior, can accurately reproduce minor loop asymmetry, a dynamic phenomenon that goes beyond static Preisach formalisms [6, 7].

Other experts have applied extensions of quasi-static models to dynamic behavior using various approaches, such as the Bertotti model based on loss separation and the Loss Surface model developed at the G2Elab. These methodologies have demonstrated the robustness of coupling quasi-static models with extension formulas across different material grades, including FeSi3% and grain-orientation.

In this work, we focus on investigating the classical Preisach model (CPM), which has been extensively studied and validated in the literature [8, 9]. The robustness of CPM was assessed by Duan et al. [9] to describe the magnetic behavior of grain-oriented silicon-iron electrical steel at various amplitudes. Some researchers have investigated hysteresis behavior under harmonic waveforms by evaluating the model's accuracy using a specific precision defined in the objective function [10, 11]. However, the effectiveness and accuracy of this model are still limited by the considerable computation time. These limitations arise from the need to perform a two-dimensional integral over the Preisach plane to evaluate the hysteresis output as well as the requirement to store the Preisach density function. Furthermore, the classical Preisach model does not inherently account for rate-dependent dynamic effects observed at higher frequency excitations [12].

To address these challenges, Everett introduced the Everett function $E(x, y)$, which integrates the Preisach density within the triangular subdomains [23], and Szabó and Füzi provided the detailed formulation and practical implementation of the

* Corresponding author: Yasmine Gabi (yasmine.gabi@izfp.fraunhofer.de).

Everett function [13]. This approach facilitates a closed-form expression of the hysteresis loop and reduces the computational complexity [13]. In addition, numerical methods based on Monte Carlo methods have been implemented to approximate the integral through random sampling in the Preisach plane. This method offers high statistical variability and enhances the numerical efficiency of the model [13, 14].

The identification of hysteresis models remains challenging in terms of both accuracy and computational time. Traditional gradient-based methods often face challenges owing to non-convex objective functions with multiple local minima [15, 16].

Because of the high-dimensional nature and non-convex properties of some hysteresis model adjustments, metaheuristic optimization methods, such as Particle Swarm Optimization (PSO), Genetic Algorithms, Ant Colony Optimization (ACO), Artificial Bee Colony algorithm (ABC), and their hybrids, have become standard practices [17–19].

In this work, we propose a novel simplified dynamic Preisach model that combines the closed-form Everett function and Monte Carlo numerical calculations. The hysteresis model parameters were investigated using two optimization methods: genetic algorithm and artificial bee colony (ABC) method. To achieve this, we characterized 80CrV2 steels under quasi-static and dynamic magnetization by analyzing minor parent hysteresis loops. The accuracy and computational efficiency of each optimization method were emphasized through a comparison of the simulated B-H loops with the experimental results.

2. THEORETICAL PREISACH MODELS

The classical Preisach model expresses the macroscopic magnetic flux density $B(t)$ as a superposition of elementary hysteresis units as follows:

$$B(t) = \iint_S \mu(\alpha,\beta)\,\gamma_{\alpha,\beta}[H(t)]\,d\alpha\,d\beta \tag{1}$$

where $\mu(\alpha,\beta)$ is the Preisach density function; $\gamma_{\alpha,\beta}[H(t)]$ represents the response of an individual unit with switching thresholds α and β; and S is the domain of the Preisach distribution [20–22].

In the traditional Preisach model, high computational effort is required for numerical integration over the full Preisach plane. Therefore, Everett et al. [23, 24] introduce the following function $E(x,y)$ to simplify the information by integrating over a specific triangular subdomain T:

$$E(x,y) = \iint_T \mu(\alpha,\beta)\,d\beta\,d\alpha \tag{2}$$

where T is defined by the operating point (x,y) and represents a portion of the Preisach plane. Using the Everett function, the magnetization can be reformulated in a piecewise manner as:

$$B(H) = \begin{cases} 0, & |H(t)| > H_m, \\ B_m - 2\,E[H_m, H(t)], & -H_m \le H(t) \le H_m, \\ & \text{and } \dfrac{dH(t)}{dt} \ge 0, \\ -B_m + 2\,E[H(t), H_m], & -H_m \le H(t) \le H_m, \\ & \text{and } \dfrac{dH(t)}{dt} < 0. \end{cases} \tag{3}$$

where H_m is the maximum applied magnetic field, and B_m is the maximum flux density. A (α_i, β_i) random sample is generated to uniformly approximate the integral within the intervals $[-H_s, H_s]$. H_s represents the input variable for the maximum magnetic field. Specifically, two independent random numbers ξ_i and ζ_i are generated and uniformly distributed in the range $[0, 1]$. They are denoted as follows:

$$\xi_i \sim U(0,1), \tag{4}$$

$$\zeta_i \sim U(0,1). \tag{5}$$

These random variables are then transformed from the interval $[0, 1]$ into the desired sampling ranges, $[-H_s, H_s]$, according to the following equations:

$$\alpha_i = -H_s + 2H_s \times \xi_i \tag{6}$$

$$\beta_i = -H_s + 2H_s \times \zeta_i \tag{7}$$

This transformation guarantees that α_i and β_i are distributed uniformly throughout the interval $[-H_s, H_s]$. Here, the probability density functions for ξ_i and ζ_i are

$$f(\xi) = \begin{cases} 1, & 0 \le \xi \le 1 \\ 0, & \text{otherwise} \end{cases} \tag{8}$$

$$f(\zeta) = \begin{cases} 1, & 0 \le \zeta \le 1 \\ 0, & \text{otherwise} \end{cases} \tag{9}$$

Using these randomly sampled points, the density function $\mu(\alpha,\beta)$ is computed for each sample. The estimated magnetic flux density $B_{\text{model}}(t)$ was then obtained by averaging the contributions from the elementary hysteresis units and applying a bias adjustment:

$$B(t) = \begin{cases} B_m + 2\,\langle I(H(t) \ge \beta)\rangle + \text{bias}, & \text{if } H(t) \ge -H_s, \\ B_m - 2\,\langle I(H(t) \le \alpha)\rangle + \text{bias}, & \text{otherwise.} \end{cases} \tag{10}$$

where $I(\cdot)$ is the indicator function, defined as:

$$I\begin{pmatrix} H(t) \ge \beta \\ H(t) \le \alpha \end{pmatrix} = \begin{cases} 1, & \text{if the condition is satisfied,} \\ 0, & \text{otherwise.} \end{cases} \tag{11}$$

The selection of the hysteron density function $\mu(\alpha,\beta)$ is crucial for the accuracy of the Preisach hysteresis B-H loops, particularly at low excitation frequencies.

Various numerical improvements have been proposed and implemented, particularly the contribution function in the

Preisach formula. The aim was to consider the physical nonlinearity and memory effects observed in ferromagnetic materials [25, 26]. We can list Lorentzian-type distributions, which are widely adopted to account for sharp transitions and long-range interactions in the coercive field space.

The Lorentzian function is expressed as follows:

$$\mu(\alpha,\beta) = ka\sqrt{a}(a+\alpha)^{-\frac{3}{2}}(a+\beta)^{-\frac{3}{2}} \tag{12}$$

This formula enables the precise modulation of the coercivity and interaction field components by adjusting the scale factor a and normalization constant k.

The Lorentzian model demonstrates robustness in dynamic simulations of soft magnetic materials, as shown by Finocchio et al. [27], who incorporated such distributions in Preisach-type operators to improve numerical convergence in low-frequency regimes. Additionally, this formula is beneficial for reproducing sharp transitions at low $B_{\max}$ values [28]. In contrast, Gaussian-type densities are more suitable for describing smooth and symmetric switching behavior. They provide excellent fitting properties for isotropic materials under periodic magnetization. In this study, the following form was considered [29, 30]:

$$\mu(\alpha,\beta) = \frac{k}{2\pi\sigma^2}\exp\left(-\frac{(\alpha-H_c)^2+(\beta-H_c)^2}{2\sigma^2}\right) \tag{13}$$

where σ denotes the spread of the switching fields, and H_c represents the average coercivity.

This approach is consistent with the findings of [31], which suggest that Gaussian-based densities improve the identification of hysteresis parameters, particularly when used in conjunction with evolutionary algorithms, such as genetic algorithms or particle swarm optimization. Additionally, for applications modeling asymmetric hysteresis behavior commonly observed under noncentered or biased magnetic excitations, exponential-type density functions offer greater flexibility [32].

Figure 1 illustrates the resulting B-H cycles in the 80CrV2 material at 100 Hz with a Gaussian density.

3. PROPOSED DYNAMIC PREISACH MODELS

To address the computational problem, the Preisach plane was discretized into a finite number of cells. The dynamic magnetic flux density loops were approximated as follows:

$$\Gamma(t) = \sum_{i=0}^{N} w_i \cdot \gamma_i\big(H(t)\big) \tag{14}$$

$\Gamma(t)$ denotes a distribution function constructed from the triangular domain of the Preisach plane. w_i are constant values that represent the contribution of each cell in the discretized Preisach plane. More specifically, w_i denotes the weight associated with the i-th discretized cell and corresponds to the integral of the Preisach density over the surface of that cell:

$$w_i = \mu(\alpha_i,\beta_i)\,\Delta\alpha\,\Delta\beta, \quad i = 1,\ldots,N. \tag{15}$$

$\gamma_i(H(t))$ denotes the corresponding elementary relay operator for each cell.

Each weight w_i corresponds to a specific physical property in a defined region of the Preisach plane. This discrete form enables accurate reconstruction of nonlinear, history-dependent B-H loops [33, 34]. CPM is known to describe quasi-static hysteresis and not explicitly account for dynamic effects, such as eddy currents, domain wall inertia, and magnetic relaxation. In the following, a modified formulation is introduced to enable the dynamic extension of the Preisach model, allowing the hysteresis behavior to be accurately reproduced under time-varying magnetic fields.

From the experimental data and various numerical tests, the $B(T)$ dynamics that best fit the measurements can be expressed as

$$B\big(H(t)\big) = \delta_0 + \delta_1\,H(t) + \delta_2\,\Gamma(H(t)) \tag{16}$$

where the coefficients δ_0, δ_1, and δ_2 are unknown parameters to be identified from experimental data.

Combining a reversible branch ($\alpha = \beta$) yields instantaneous, memory free response and an irreversible branch ($\alpha > \beta$) retaining memory and saturation. Hybrid neural-Preisach architectures using this two-branch structure accurately reproduce dynamic B-H loops under harmonic or time-varying fields [35, 36]. A hysteron state function $\gamma_{(\alpha,\beta)}(H(t))$ is defined as follows:

$$\gamma_{(\alpha,\beta)}(H(t)) = \begin{cases} +1, & \text{if } H(t) \geq \beta, \\ -1, & \text{if } H(t) \leq \alpha, \end{cases} \tag{17}$$

The experimental flux density data B_{exp} contains n points per excitation period. Five excitation frequencies are used: 30 Hz, 50 Hz, 180 Hz, 250 Hz, and 400 Hz. Each frequency has a corresponding period $T_f = 1/f$. The time step for numerical integration is set as

$$\Delta t = \frac{T_f}{n} \tag{18}$$

The simulation proceeds in discrete time steps $t_i = i\Delta t$ (where $i = 0, 1, 2, \ldots, n-1$). At each step, the output $B(H(t_i))$ is computed according to

$$B(H(t)) = \delta_0 + \delta_1\,H(t) + \delta_2 \iint_{\alpha\geq\beta} \mu(\alpha,\beta)\;\gamma_{(\alpha,\beta)}(H(t))\;d\alpha\,d\beta \tag{19}$$

Here, the model function reproduces the switching behavior of hysterons, effectively capturing the nonlinearity and memory effects that reflect the transition between magnetization states. Eq. (19) shows that the model parameters (δ_0, δ_1 and δ_2), as well as the Preisach density $\mu(\alpha,\beta)$, are independent of the excitation frequency f. The frequency only appears in the input $H(t) = H_m \sin(2\pi f t)$. For numerical implementation, the continuous Preisach integral in Eq. (19) is discretized into $N = 5000$ elementary cells and approximated by a finite weighted sum in Eq. (14).

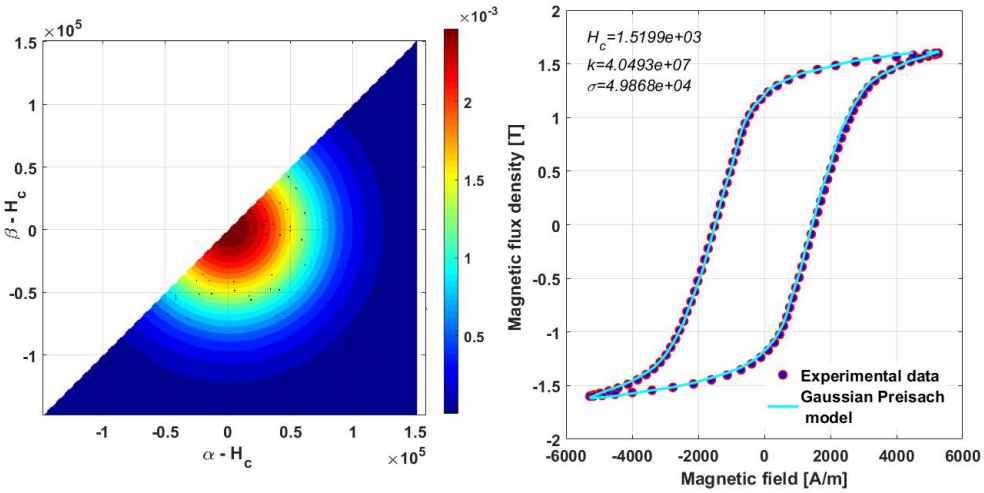

FIGURE 1. Correspondence between Gaussian distribution in Preisach plane and hysteresis loops at 100 Hz.

4. PARAMETER IDENTIFICATION ALGORITHMS

The model is characterized by a parameter vector $\boldsymbol{\theta} = [k, \sigma, H_c, \delta_0, \delta_1, \delta_2]$. The difference between the experimental and simulated magnetic flux densities was quantified using the quadratic error function:

$$I(\theta) = \frac{1}{n}\sqrt{\sum_{i=1}^{n}\left(B_{\exp,i} - B_{\text{model},i}\right)^2} \tag{20}$$

4.1. Artificial Bee Colony (ABC) algorithm

The Artificial Bee Colony (ABC) algorithm is known to be a robust evolutionary optimization method that mimics the foraging behavior of honeybees [37] and involves the following steps, which are summarized in the flowchart of Figure 2:

- Step 1: Define the population size, maximum number of iterations, and error tolerance. Generate an initial population of candidate solutions θ randomly within the predefined bounds.
- Step 2: Each employed bee explores the neighborhood of its candidate solution by generating a new solution θ^j using the update rule

$$\theta^j \leftarrow \theta^j + \delta\theta^j \tag{21}$$

  where $\delta\theta$ denotes a random perturbation. The objective function (Eq. (18)) is evaluated for each new candidate. If the new candidate reduces the error, it replaces the previous solution.
- Step 3: Onlooker bees select promising candidates based on their fitness inversely proportional to the error and explore their neighborhoods to generate new solutions, updating them if improvements are found.
- Step 4: If a candidate solution does not improve over a specified number of iterations, it is abandoned and replaced by a new randomly generated candidate to maintain the diversity and avoid local minima.

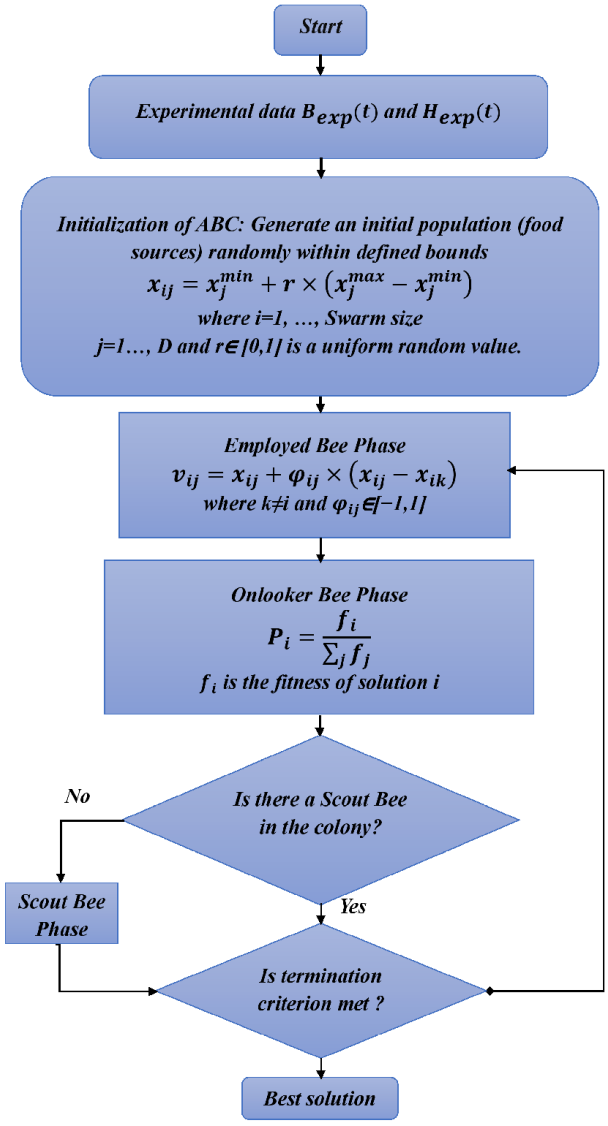

FIGURE 2. Schematic flowchart of the Artificial Bee Colony (ABC) method.

- Step 5: Evaluate if the best candidate's error is below the predefined tolerance or if the maximum number of iterations has been reached. If either condition is met, the algorithm terminates; otherwise, it returns to the employed bee phase.
- Step 6: The best candidate solution is selected as the optimal parameter vector θ that minimizes objective function $I(\theta)$.

Table 1 summarizes the principal control parameters of the ABC algorithm. These parameter settings follow widely reported values in previous studies [37, 38] and were additionally confirmed through preliminary simulations to guarantee reliable convergence and optimization stability.

TABLE 1. ABC algorithm control parameters.

Parameter	Value	Description
Colony size	40–60	Employed + onlooker bees
Trial limit	100	Abandonment threshold
Employed bees	20–30	Exploration phase
Onlooker bees	20–30	Exploitation phase
Maximum cycles	200–500	Termination criterion

4.2. Genetic Algorithm

In this parameter-fitting algorithm, the genetic algorithm takes the measured waveform of the applied field with the corresponding flux density as input (see flowchart in Figure 3). It also requires an initial guess vector $\theta_0 = [k_0, \sigma_0, H_{c,0}, \delta_{0,0}, \delta_{1,0}, \delta_{2,0}]$. These parameters are bounded in the interval, and the lower and upper bounds $[b_l, b_u]$ must be selected. In addition, the GA setup control parameters included a population size of 100, a limit of 3000 generations, five elite individuals preserved in each generation, 0.8 crossover probability, an adaptive feasible mutation operator, and a convergence tolerance of 10^{-6}. In return, the GA outputs the best parameter vector θ_0 it found that minimizes the fit error, a value denoted as the best objective, and computes the final root mean square error (RMSE) between the final simulated $B_{\text{model}}(t)$ and the measured B_{exp}:

- Step 1: Initialization: $t \leftarrow 0$ and randomly initialize a population $P[0]$ of 100 candidate vectors sampled uniformly within $[b_l, b_u]$.
- Step 2: Fitness Evaluation of Initial Population: For every candidate θ in $P[0]$: simulate B_{model}, compute the fitness, and retain the best fitness obtained thus far.
- Step 3: Iterative Genetic Evolution: While $t <$ maximum number of generations and best fitness $>$ convergence tolerance, do:
  - a) Selection: Automatically copy the top elite count individuals with the lowest fitness into the new generation and fill the remaining slots in the parent pool via selection strategies biased toward better fitness.

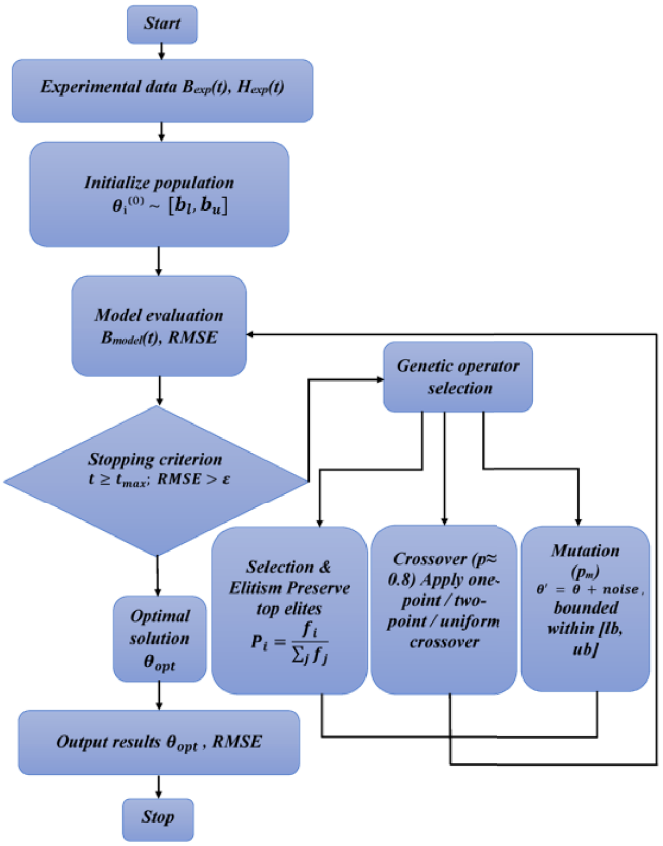

FIGURE 3. Schematic flowchart of the Genetic Algorithm (GA).

  - b) Crossover: With probability 0.8 per parent pair, execute gene crossover (single-point, two-point, or uniform) to produce offspring.
  - c) Mutation: Apply adaptive feasible mutation with a defined probability to keep offspring within $[b_l, b_u]$, preserving diversity.
  - d) Evaluate Offspring: For new individual, simulate B_{model} and compute its fitness, as in Step 2.
  - e) Update Population: Merge elite individuals from the previous generation with the newly evaluated offspring, sort by fitness, and choose the top population size vectors to form $P[t+1]$.
  - f) Track Best: Update the overall best objective and its corresponding θ if a better candidate is identified.
  - g) $t \leftarrow t+1$
- Step 4: The parameter vector θ that achieves the lowest objective across all generations is the best objective value for θ.
- Step 5: Simulate the final B_{model}, compute the RMSE, and save together with θ.

5. RESULTS AND DISCUSSION

To evaluate the robustness of both metaheuristic algorithms on the Preisach dynamic model, it is essential to utilize measurement data. The magnetic properties of materials are assessed

TABLE 2. Chemical composition of 80CrV2 material.

Material	C	Si	Mn	P_{max}	S_{max}	Cr	Mo	Ni	V
80CrV2	0.75–0.85	Max 0.4	0.30–0.50	0.025	0.025	0.4–0.6	Max 0.1	Max 0.4	0.15–0.25

TABLE 3. Comparative identified parameters of the Gaussian Preisach model using GA and ABC algorithms under different excitation conditions.

Parameter	Identified values (GA/ABC)										Unit
	30 Hz		50 Hz		180 Hz		250 Hz		400 Hz		
	0.6 T	1.6 T	0.6 T	1.6 T	0.6 T	1.6 T	0.6 T	1.6 T	0.6 T	1.6 T	
H_c	6.43/6.65	6.40/6.85	6.82/7.25	11.3/12.1	9.35/10.2	20.3/22.2	10.6/11.8	24.8/27.5	12.9/14.6	36.1/39.5	A/m $\times 10^2$
k	2.98/3.15	2.72/2.95	2.06/2.28	2.28/2.45	0.84/0.96	1.37/1.58	1.23/1.42	0.49/0.61	3.22/3.55	3.23/3.60	$-\times 10^5$
σ	3.29/3.75	1.53/1.92	1.42/1.78	2.09/2.48	3.70/4.15	3.32/3.85	2.44/2.85	2.40/2.95	3.41/3.95	0.52/0.71	A/m $\times 10^7$
δ_0	5.06/5.55	3.05/3.65	5.04/5.60	3.07/3.72	4.57/5.05	3.04/3.58	4.18/4.70	2.97/3.45	3.53/4.10	2.85/3.20	$-\times 10^{-4}$
δ_1	2.97/3.45	7.53/8.60	0.79/1.15	6.23/7.10	0.58/0.82	8.96/10.2	5.16/6.20	1.43/1.95	5.16/6.40	10.0/11.5	$-\times 10^3$
δ_2	6.86/7.80	4.66/5.40	2.83/3.55	1.02/1.65	3.96/4.80	4.19/4.95	1.48/2.10	3.62/4.35	3.67/4.45	0.19/0.38	$-\times 10^3$

using an Epstein frame, in accordance with DIN-EN 10252 and DIN-EN 60404-2 standards. This method allows for the determination of the hysteresis behavior of a set of strips, with a minimum of four samples required for accurate measurement. To ensure that the material properties in the tested area remain unchanged, the specimens are precisely laser-cut from strip steel. The chemical composition of 80CrV2 material grades is detailed in Table 2.

The measurement setup consists of a Brockhaus Epstein frame system. The technical data of the system are detailed in following:

- Specimen dimensions: The samples are cut to the following dimensions: 99.79 mm × 9.72 mm × 1.6 mm.
- Primary coil ($n_1 = 180$ turns): Generates the magnetic field within the sample.
- Secondary coil ($n_2 = 180$ turns): Detects voltage and calculates the magnetic flux density B.
- Frequency range: DC up to 5 kHz.
- Field Intensity: 1 to 24 kA/m.
- Magnetic flux density: 0.001 up to 2 T.
- The magnetic path length is $l = 399.16$ mm.
- The sampling rate was set dynamically to a thousand samples per excitation period.

A detailed study evaluated and compared two optimization strategies for the identification of the Preisach hysteresis model parameters. We selected two stochastic optimization methods. The most commonly used algorithms are genetic methods, which are based on evolutionary mechanisms for global solution investigation, and the ABC method, which is based on the swarm-inspired exploration for complex functions. The convergence of the two distinct optimization algorithms was analyzed in terms of the comparative efficiency and minimization of the total error across successive iterations (see Figure 4). The optimization algorithms were developed in the MATLAB environment, combining Monte Carlo integration with 5000 samples to calculate the dynamic B(H) curve of Preisach (see Figure 5). It can be noticed that the ABC algorithm effectively reduced the quadratic error by achieving convergence with an R^2 value higher than 0.99 across various excitation levels.

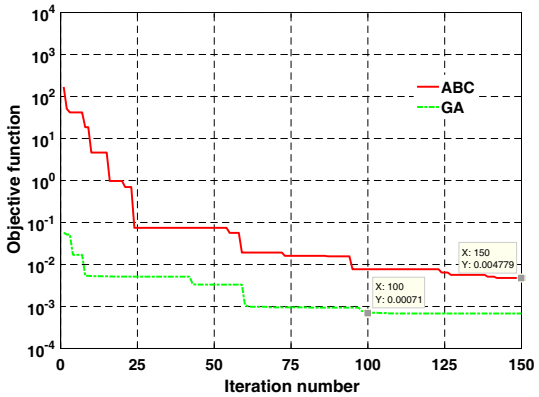

FIGURE 4. Total error depending on the number of iterations.

The Genetic Algorithm (GA) exhibited good performance in terms of lower error levels with a modest number of 80 iterations. The Artificial Bee Colony (ABC) algorithm displays an impressive convergence rate, progressively reducing the error over successive iterations. This behavior is indicative of swarm intelligence approaches, which rely on the collective perception of agents to search efficiently in the solution space. Table 3 presents the parameters identified using the GA with a Gaussian Preisach density. The parameter identification was carried out independently for each excitation frequency using the cor-

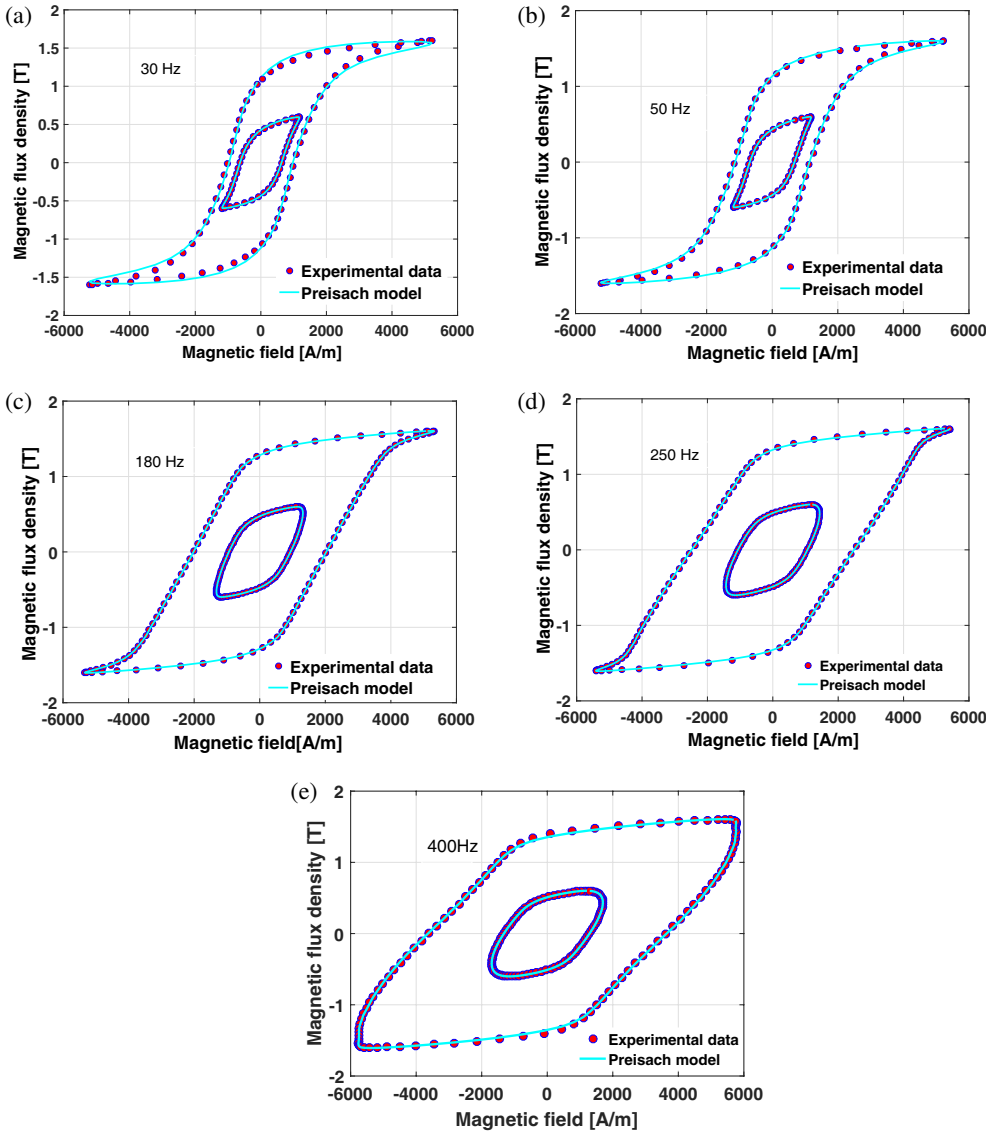

FIGURE 5. Major and minor hysteresis loops at different excitation frequencies.

TABLE 4. Comparison of the total errors obtained using GA and ABC algorithms at different excitation frequencies and magnetic flux density levels.

Frequency	$B_{max} = 0.6$ T		$B_{max} = 1.6$ T	
	GA	ABC	GA	ABC
30 Hz	0.00400	0.00685	0.02214	0.03120
50 Hz	0.00272	0.00510	0.01099	0.01845
180 Hz	0.00271	0.00492	0.00850	0.01480
250 Hz	0.00147	0.00375	0.00506	0.00960
400 Hz	0.00071	0.00477	0.00412	0.01695

responding experimental hysteresis loop. This strategy allows the model to accurately capture frequency-dependent dynamic effects. The variation of these parameters with frequency reflects the effective dynamic magnetic behavior rather than intrinsic static material properties. For validation purposes, an additional identification was performed using an ABC under the same excitation conditions. Although both methods lead to comparable parameter values, the GA systematically yields a much smaller error. Table 4 summarizes the comparative performance of the two methods, quantitatively evaluating their efficiency in terms of the final error.

Overall, the metaheuristic algorithms GA outperformed ABC in terms of final accuracy, with GA emerging as the most effective optimization method. Its quick error reduction and ability to maintain a low error level with fewer iterations highlights its efficiency and robustness in complex optimization problems. The ABC algorithm is less efficient than GA, and GA achieves higher final accuracy, but it requires more iterations and greater computational effort.

6. CONCLUSION

The study addresses a simplified dynamic Preisach hysteresis model that combines a closed-form Everett function with Monte Carlo integration. A Gaussian Preisach density and a

reduced-order Everett representation are employed to reduce computational effort while preserving the key nonlinear and history-dependent features of B-H magnetic hysteresis.

To identify the model parameters, the authors employ Genetic Algorithms (GA) and Artificial Bee Colony (ABC). For this purpose, experimental B-H loops of 80CrV2 steel were measured and used in the identification procedure. Both optimization methods show very good agreement with the experimental data: the magnetic response of the ferromagnetic material is accurately reproduced at various operating points and frequencies, with determination coefficients $R^2 > 0.99$. However, GA consistently achieves lower errors and faster convergence, making it the preferred method when high accuracy is needed.

Future work will investigate the robustness of this new Preisach modeling approach compared with existing methods from the literature in terms of computational time, accuracy, and ease of implementation in numerical codes. Further research will aim for extending the model toward fully frequency-continuous formulations suitable for arbitrary waveforms with higher harmonics, as well as for comparing the robustness of the model with other state of the art models to reproduce the magnetic responses on one-material grades.

ACKNOWLEDGEMENT

Parts of this scientific work were funded by the DFG within the research program BE 1691/291-1|WO 903/5-1.

REFERENCES

[1] Jiles, D. C. and D. L. Atherton, "Theory of ferromagnetic hysteresis," *Journal of Magnetism and Magnetic Materials*, Vol. 61, No. 1-2, 48–60, Sep. 1986.

[2] Jiles, D. C., "Frequency dependence of hysteresis curves in conducting magnetic materials," *Journal of Applied Physics*, Vol. 76, No. 10, 5849–5855, 1994.

[3] Regan, A., J. Wilson, and A. J. Peyton, "Extension to the Jiles-Atherton hysteresis model using gaussian distributed parameters for quenched and tempered engineering steels," *Sensors (Basel, Switzerland)*, Vol. 25, No. 5, 1328, Feb. 2025.

[4] She, S., X. Pang, J. Liu, X. Zheng, K. Yu, X. Zou, R. Zhu, R. Guo, and W. Yin, "Fast inversion of parameters on Jiles-Atherton hysteresis model based on physics-guided deep learning network," *Engineering Applications of Artificial Intelligence*, Vol. 157, 111233, Oct. 2025.

[5] Zirka, S. E., Y. I. Moroz, P. Marketos, and A. J. Moses, "Viscosity-based magnetodynamic model of soft magnetic materials," *IEEE Transactions on Magnetics*, Vol. 42, No. 9, 2121–2132, Sep. 2006.

[6] Zirka, S. E., Y. I. Moroz, S. Steentjes, K. Hameyer, K. Chwastek, S. Zurek, and R. G. Harrison, "Dynamic magnetization models for soft ferromagnetic materials with coarse and fine domain structures," *Journal of Magnetism and Magnetic Materials*, Vol. 394, 229–236, 2015.

[7] Wang, T., M. Noori, W. A. Altabey, Z. Wu, R. Ghiasi, S.-C. Kuok, A. Silik, N. S. D. Farhan, V. Sarhosis, and E. N. Farsangi, "From model-driven to data-driven: A review of hysteresis modeling in structural and mechanical systems," *Mechanical Systems and Signal Processing*, Vol. 204, 110785, 2023.

[8] Mayergoyz, I., "Mathematical models of hysteresis," *IEEE Transactions on Magnetics*, Vol. 22, No. 5, 603–608, Sep. 1986.

[9] Duan, N., X. Gao, L. Zhang, W. Xu, S. Huang, M. Lu, and S. Wang, "An improved Preisach model for magnetic hysteresis of grain-oriented silicon steel under PWM excitation," *Applied Sciences*, Vol. 14, No. 1, 321, 2024.

[10] Antonio, S. Q., F. R. Fulginei, A. Laudani, A. Faba, and E. Cardelli, "An effective neural network approach to reproduce magnetic hysteresis in electrical steel under arbitrary excitation waveforms," *Journal of Magnetism and Magnetic Materials*, Vol. 528, 167735, 2021.

[11] Xiao, S. and Y. Li, "Modeling and high dynamic compensating the rate-dependent hysteresis of piezoelectric actuators via a novel modified inverse preisach model," *IEEE Transactions on Control Systems Technology*, Vol. 21, No. 5, 1549–1557, Sep. 2013.

[12] Ramirez-Laboreo, E., M. G. L. Roes, and C. Sagues, "Hybrid dynamical model for reluctance actuators including saturation, hysteresis, and eddy currents," *IEEE/ASME Transactions on Mechatronics*, Vol. 24, No. 3, 1396–1406, 2019.

[13] Szabó, Z. and J. Füzi, "Implementation and identification of Preisach type hysteresis models with Everett function in closed form," *Journal of Magnetism and Magnetic Materials*, Vol. 406, 251–258, 2016.

[14] Jiles, D. and D. Atherton, "Ferromagnetic hysteresis," *IEEE Transactions on Magnetics*, Vol. 19, No. 5, 2183–2185, Sep. 1983.

[15] Yang, L., B. Ding, W. Liao, and Y. Li, "Identification of preisach model parameters based on an improved particle swarm optimization method for piezoelectric actuators in micromanufacturing stages," *Micromachines*, Vol. 13, No. 5, 698, Apr. 2022.

[16] Yao, J., X. Luo, F. Li, J. Li, J. Dou, and H. Luo, "Research on hybrid strategy Particle Swarm Optimization algorithm and its applications," *Scientific Reports*, Vol. 14, No. 1, 24928, Oct. 2024.

[17] Sedira, D., Y. Gabi, A. Kedous-Lebouc, K. Jacob, B. Wolter, and B. Strass, "A comparison between ABC method and PSO method for Hysteresis Parameter determination," in *25th Soft Magnetic Materials Conference (SMM'2022)*, hal–03 676 283, Grenoble, France, 2022.

[18] Sedira, D., Y. Gabi, A. Kedous-Lebouc, K. Jacob, B. Wolter, and B. Straß, "ABC method for hysteresis model parameters identification," *Journal of Magnetism and Magnetic Materials*, Vol. 505, 166724, Jul. 2020.

[19] Gabi, Y., K. Jacob, B. Wolter, C. Conrad, B. Strass, and J. Grimm, "Analysis of incremental and differential permeability in NDT via 3D-simulation and experiment," *Journal of Magnetism and Magnetic Materials*, Vol. 505, 166695, Jul. 2020.

[20] Mayergoyz, I. D., *Mathematical Models of Hysteresis*, 1–207, Springer-Verlag, 1991.

[21] Szabó, Z. and J. Füzi, "Preisach type hysteresis models with Everett function in closed form," in *Proceedings of the COMPUMAG 20th Conference on the Computation of Electromagnetic Fields*, Montreal, Canada, 2015.

[22] Szabó, Z., I. Tugyi, G. Kádár, and J. Füzi, "Identification procedures for scalar preisach model," *Physica B: Condensed Matter*, Vol. 343, No. 1–4, 142–147, 2004.

[23] Everett, D. H., "A general approach to hysteresis. Part 4. An alternative formulation of the domain model," *Transactions of the Faraday Society*, Vol. 51, 1551–1557, 1955.

[24] Bertotti, G., "Generalized Preisach model for the description of hysteresis and eddy current effects in metallic ferromagnetic materials," *Journal of Applied Physics*, Vol. 69, No. 8, 4608–4610,

Apr. 1991.

[25] Mörée, G. and M. Leijon, "Review of hysteresis models for magnetic materials," *Energies*, Vol. 16, No. 9, 3908, 2023.

[26] De Santis, V., A. D. Francesco, and A. G. D'Aloia, "A numerical comparison between Preisach, J-A and D-D-D hysteresis models in computational electromagnetics," *Applied Sciences*, Vol. 13, No. 8, 5181, Apr. 2023.

[27] Finocchio, G., M. Carpentieri, B. Azzerboni, C. Ampelli, and G. Maschio, "An isotropic analytical vector Preisach model based on the Lorentzian function," *Physica Status Solidi (C)*, Vol. 1, No. 12, 3740–3743, Dec. 2004.

[28] Azzerboni, B., E. Cardelli, E. D. Torre, and G. Finocchio, "Reversible magnetization and lorentzian function approximation," *Journal of Applied Physics*, Vol. 93, No. 10, 6635–6637, May 2003.

[29] Pruksanubal, P., A. Binner, and K. H. Gonschorek, "Determination of distribution functions and parameters for the preisach hysteresis model," in *2006 17th International Zurich Symposium on Electromagnetic Compatibility*, 258–261, Singapore, 2006.

[30] Evans, P. G. and M. J. Dapino, "Measurement and modeling of magnetic hysteresis under field and stress application in iron-gallium alloys," *Journal of Magnetism and Magnetic Materials*, Vol. 330, 37–48, Mar. 2013.

[31] Xiao, K., Z. Wang, H. Wang, J. Sun, Y. Zheng, and Y. Huang, "A precision-drive hysteresis model with an equal-density weight function for GMA feedforward compensation," *Nanotechnology and Precision Engineering*, Vol. 6, No. 2, 023002, Mar. 2023.

[32] Yu, S., H. Li, J. Sun, and Z. Wang, "Accurate fitting of Preisach model parameters using GMM with non-uniform grid partition," *Measurement Science and Technology*, Vol. 36, No. 4, 046126, 2025.

[33] Peng, D., W. Sima, M. Yang, M. Zou, Y. Zhou, and Y. Liu, "An improved centered cycle method for identifying the Preisach distribution function," *IEEE Transactions on Magnetics*, Vol. 54, No. 11, 1–5, Nov. 2018.

[34] Li, X., D. Kim, S. M. Neumayer, M. Ahmadi, and S. V. Kalinin, "Estimating Preisach density via subset selection," *IEEE Access*, Vol. 8, 61 767–61 774, 2020.

[35] Zhao, H., X. Zhao, S. Xu, W. Liu, Y. Wu, and Y. An, "Hysteresis and loss characteristics of soft magnetic materials based on nonlinear Preisach model," *Journal of Superconductivity and Novel Magnetism*, Vol. 36, No. 7, 1655–1664, 2023.

[36] Melo, P. and R. E. Araújo, "An overview on Preisach and Jiles-Atherton hysteresis models for soft magnetic materials," in *8th Doctoral Conference on Computing, Electrical and Industrial Systems (DoCEIS)*, 398–405, Costa de Caparica, Portugal, 2017.

[37] Gabi, Y., K. Jacob, and K. Szielasko, "Parameters optimization of the chemical reaction hysteresis model using genetic algorithms and the artificial bee colony method," *Progress In Electromagnetics Research C*, Vol. 158, 19–25, 2025.

[38] Li, Y., L. Li, X. Yang, and B. Zhao, "Flexible job shop scheduling based on energy consumption of method research," *IEEE Access*, Vol. 13, 127 885–127 901, 2025.